

Molecular and impedance spectroscopy of $\text{Na}_2\text{Mo}_2\text{O}_7$ ceramics

SUBRAT KUMAR BARIK^{1,*}, SANDEEP CHATTERJEE² and
R N P CHOUDHARY³

¹Department of Physics, National Institute of Technology Silchar, Silchar 788 010, India

²Jawaharlal Nehru University, New Delhi 110 067, India

³Department of Physics, ITER, SOA University, Bhubaneswar 751 030, India

*Corresponding author. E-mail: subrat.nits@gmail.com

MS received 19 March 2013; revised 30 January 2014; accepted 11 February 2014

DOI: 10.1007/s12043-014-0803-9; ePublication: 27 September 2014

Abstract. The fine (i.e. 38 nm) powder of polycrystalline $\text{Na}_2\text{Mo}_2\text{O}_7$ was prepared by the high-temperature solid-state reaction technique. The formation of the compound in orthorhombic system is confirmed by preliminary structural analysis using X-ray diffraction (XRD) data. Spectroscopic studies of the compound have been carried out by vibration spectroscopy (Raman/FTIR) to understand its molecular structure at microscopic level. The complex impedance spectroscopy (CIS) technique has been used to study the electrical properties of the material as a function of frequency (10^2 – 10^6 Hz) at different temperatures (23–450°C), and also to investigate the fundamental mechanism involved in the material. Impedance analysis also indicates that below 300°C, the electrical conduction in the material is due to grain interior only. At and above 325°C, the contribution of grain boundary is clearly evident. The electrical processes in the material are found to be temperature-dependent and are due to the relaxation phenomena in it. A frequency-dependent maximum of the imaginary electrical impedance is found to obey the Vogel–Fulcher law.

Keywords. X-ray diffraction; impedance spectroscopy; electrical conduction; relaxation phenomena.

PACS No. 61.05.cp

1. Introduction

Though a large number of ceramic oxides having different structures have been developed (synthesis and characterization) in the past, some layered and structured oxides with microstructure of oxygen octahedra or tetrahedra have been the subject of extensive investigation because of their various industrial and technological applications. Amongst them, molybdates of different structural families have drawn considerable attention of

the researchers because of their wide-ranging properties such as phase transition over a range of temperature, low dielectric constant, high dielectric loss and high electrical conductivity [1,2]. Interestingly, presence of a vacant *d*-shell in the molybdenum group is fascinating, as it adds charge transfer within the molybdate groups from oxygen atoms to the central molybdenum atom in the excited state. This imparts a number of advantageous optical properties, viz. strong absorption, luminescence, etc. and electrical properties on the molybdates that make it a potential candidate for use in high-energy electromagnetic, calorimetric and radiation detection devices [3,4]. It is interesting to observe that some compounds with the chemical formula A_2BX_4 (A = alkali metal ions or equivalent monovalent complex ions, BX_4 = divalent tetrahedral complex, i.e. SO_4^{-2} , SeO_4^{-2} , $ZnBr_4^{-2}$ etc.) undergo successive phase transitions from a low-temperature commensurate (ferroelectric) phase to a high-temperature normal (paraelectric) phase [5–7]. It is difficult to grow large single crystals of the above compounds because most of the lithium and sodium molybdates and tungstates are moisture-sensitive or hygroscopic in nature [8]. Therefore, solid-state reaction technique has been used to prepare $Na_2Mo_2O_7$ for studying its molecular and impedance spectroscopic properties in different experimental conditions. It is noted that the above properties of the material have not been reported so far.

2. Experimental

The polycrystalline sample of $Na_2Mo_2O_7$ was prepared by a solid-state reaction technique using high-purity ingredients: Na_2CO_3 and MoO_3 (99.9%, s.d. Fine Chemical Pvt. Ltd., India) and WO_3 (99.5%, BDH Chemicals Ltd., England) in the required stoichiometry. The ingredients of the desired compound were thoroughly mixed in an agate mortar for 5 h. The mixed powder was calcined in air atmosphere in an alumina crucible at $550^\circ C$ for 6 h. The process of grinding and calcination was repeated until the formation of the compound was confirmed by room-temperature X-ray diffraction (XRD) data. The repeated recalcined homogeneous powder was used to make cylindrical pellets of 10 mm diameter and 1–2 mm thickness, at a pressure of 4×10^7 N/m² using a hydraulic press. Polyvinyl alcohol was used as a binder. The pellets were sintered in air at $590^\circ C$ for 6 h. The organic binder burnt off during the sintering process. The polished and parallel surface of pellets were electroded with high purity silver paste, and then dried at $150^\circ C$ in an oven for 3 h, before taking electrical measurements. For preliminary structural studies, the X-ray diffractogram of $Na_2Mo_2O_7$ was done at room temperature ($23^\circ C$) using a Philips (PW 1710, Holland) X-ray powder diffractometer with $CoK\alpha$ radiation ($\lambda = 1.7902 \text{ \AA}$) in a wide range of Bragg angles 2θ ($20^\circ < 2\theta < 80^\circ$) at a scanning rate of $2^\circ/\text{min}$. The surface morphology of the gold-sputtered pellet sample was recorded at different magnifications at room temperature using a JEOL-JSM (S80) scanning electron microscope (SEM). The dielectric constant (ϵ) and tangent loss ($\tan \delta$) of the compound were measured as functions of frequency (100 Hz–100 kHz) at different temperatures (23– $450^\circ C$) using a HioKi 3532 LCR Hitester capacitor measuring assembly. A laboratory-made sample holder was used for the measurements. The temperature of the sample was recorded using a chromel–alumel thermocouple having an accuracy of $\pm 1^\circ C$.

3. Results and discussion

3.1 X-ray diffraction analysis

The X-ray diffractogram of anhydrous $\text{Na}_2\text{Mo}_2\text{O}_7$ recorded at room temperature is shown in figure 1.

The sharp and single diffraction peaks of XRD pattern, which are quite different from those of the constituent materials, suggest the formation of a new single-phase compound. The XRD peaks were indexed using the standard computer program package, POWD [9]. Subsequent calculations and refinements have shown that $\text{Na}_2\text{Mo}_2\text{O}_7$ has orthorhombic unit cell with Cmca space group. The least-squared refined unit cell parameters of the compound (with estimated error in parenthesis) are: $a = 7.1642(16)$, $b = 11.8371(16)$, $c = 14.7143(16)$ Å and volume (V) = 1247.75 Å³. The crystallite size (P_{hkl}) of the sample was calculated from the broadening of the reflection peaks (figure 1) using Scherrer's equation [10],

$$P_{hkl} = \frac{0.89\lambda}{\beta_{1/2} \cos \theta_{hkl}}$$

where $\beta_{1/2}$ is the peak width of reflection at half height, θ_{hkl} is the Bragg's angle and λ is the wavelength of X-ray used ($\lambda = 1.7902$ Å). The average crystallite size was found to be 38 nm.

3.2 Vibrational (Raman/FTIR) spectrum analysis

Analysis of Raman/FTIR spectra has been carried out to determine the molecular structure of the compound at microscopic level, and also to confirm its formation.

Raman spectrum of one of the compounds (for illustration; viz. anhydrous $\text{Na}_2\text{Mo}_2\text{O}_7$) recorded at room temperature in the region of 200 – 1000 cm^{-1} are shown in figure 2a. FTIR spectrum of the same material in the region of interest is shown in figure 2b. The vibrational bands observed for the materials match well with the spectrum reported earlier [11,12] providing further evidence of the formation of the compounds. An empirical assignment of frequencies to the different modes of vibrations of different

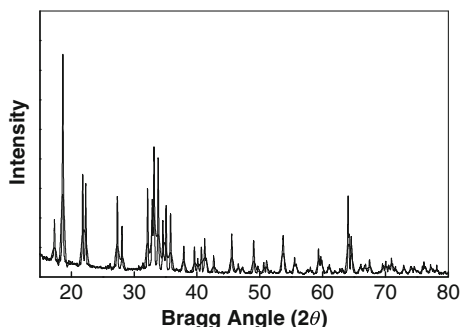


Figure 1. X-ray diffractogram of $\text{Na}_2\text{Mo}_2\text{O}_7$ recorded at room temperature.

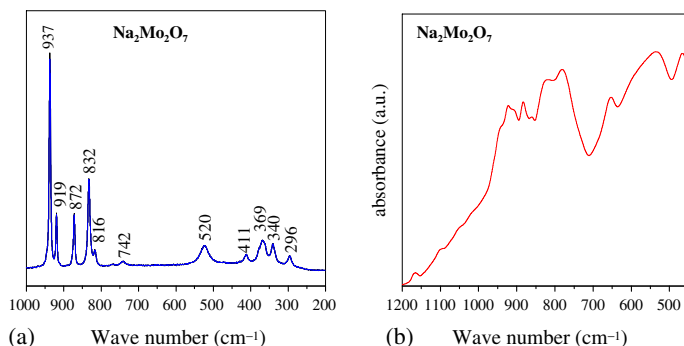


Figure 2. Room-temperature (a) Raman spectra and (b) FTIR spectra of $\text{Na}_2\text{Mo}_2\text{O}_7$.

structural groups in the materials is given in table 1. The spectral patterns and the corresponding band assignments of $\text{Na}_2\text{Mo}_2\text{O}_7$ show a very close analogy with those of $\text{K}_2\text{Cr}_2\text{O}_7$, $\text{Na}_4\text{P}_2\text{O}_7$ and $\text{Na}_4\text{V}_2\text{O}_7$ [13]. This suggests the possibility of the vibrations of the bridging Mo–O–Mo bonds with two MoO_3 groups located symmetrically with respect to the Mo–O–Mo bridge. This presents a C_{2v} symmetry with a structure $\text{O}_3\text{Mo–O–MoO}_3$ suggesting a coordination of tetrahedrons of MoO_4 and octahedrons of MoO_6 [11,12].

3.3 Impedance spectrum analysis

In order to carry out the detailed studies of electrical properties of the compound and its temperature dependence on frequency, impedance spectroscopy has been employed. It is necessary to understand the contribution of grain, grain boundary and ceramic interface effects, which greatly influence the electrical properties (in an applied alternating field).

Table 1. Vibrational band (Fourier transform infra-red and Raman spectra) assignments

FTIR			Raman		
Peaks (cm^{-1})	Assignment		Peaks (cm^{-1})	Assignment	
466	ν_s (Mo–O–Mo)	Symmetric str.	296	δ (Mo–O–Mo)	Bending mode
536	ν_s (Mo–O–Mo)	Symmetric str.	340		
653	δ (Mo–O–Mo)	Bending mode	369		
781	ν_{as} (Mo–O–Mo/ $\text{O}_3\text{Mo–O–MoO}_3$)	Asymmetric str.	411	ν_s (Mo–O–Mo)	Symmetric str.
883	ν_{as} (MoO_4)	Asymmetric str.	520		
922	ν_s (MoO_4)	Symmetric str.	742	ν_{as} (Mo–O–Mo)	Asymmetric str.
			816		
			832	ν_s (MoO_4)	Symmetric str.
			872		
			919	ν_{as} (MoO_4)	Asymmetric str.
			937		

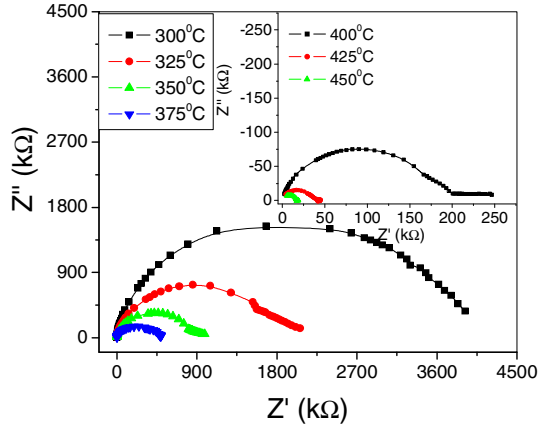


Figure 3. Complex impedance spectrum (Nyquist plot) at different temperatures.

Figure 3 shows a set of impedance data of $\text{Na}_2\text{Mo}_2\text{O}_7$ taken over a wide frequency range at different temperatures as a Nyquist diagram (complex impedance spectrum). The grain (bulk) contribution appears significant in the material and a semicircle can be observed up to 300°C. Again, on increasing the temperature, the grain boundary contributions become dominant over the bulk properties in the material, and thus, two semicircles can be traced. Hence, grain and grain boundary effects can be separated at these temperatures. It can also be seen from the plots (figure 3) that the values of both grain and grain boundary resistances decrease with an increase in temperature, supporting the NTCR-type behaviour of $\text{Na}_2\text{Mo}_2\text{O}_7$ [13,14].

The frequency dependence of the imaginary part (Z'') of complex impedance of $\text{Na}_2\text{Mo}_2\text{O}_7$ at various temperatures is shown in figure 4. The temperature strongly affects the magnitude of resistance (the value of Z'' decreases with increasing temperature). The

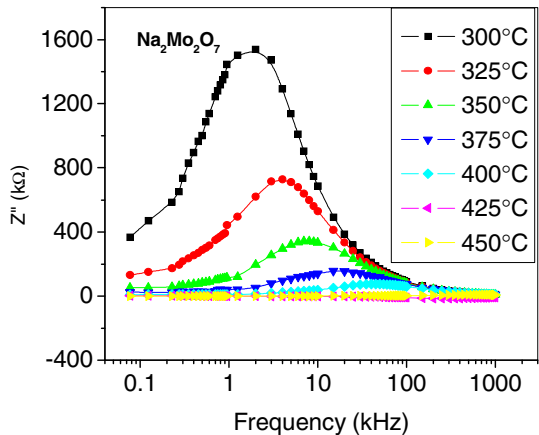


Figure 4. Frequency variation of imaginary impedance (Z'') of $\text{Na}_2\text{Mo}_2\text{O}_7$ at different temperatures.

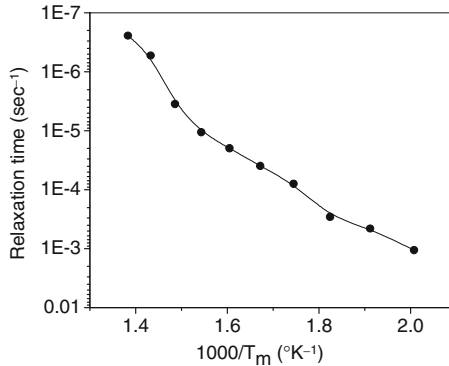


Figure 5. Variation of relaxation time (τ) with temperature.

spectrum of Z'' at each temperature exhibits one relaxation peak. The peak position shifts to higher frequency side on increasing the temperature. Figure 5 shows the relaxation time (τ) as a function of temperature T_m . It is well known that the frequency dependence of T_m in relaxor ferroelectrics cannot be described by simple Arrhenius law, which is to be expected for Debye-type relaxation process, but instead this dependence obeys the Vogel–Fulcher law [15], when ω_m depends on temperature. In order to analyse the relaxation features of $\text{Na}_2\text{Mo}_2\text{O}_7$ ceramics the experimental data of τ ($=1/2\pi f$) vs. $10^3/T_m$ was modelled using the Vogel–Fulcher relationship:

$$f = f_0 \exp[-E_a/k_B(T_m - T_f)],$$

where f is the operating frequency, f_0 is the attempt frequency, E_a is the activation energy, T_f is the static freezing temperature and k_B is the Boltzmann constant. It is observed from the figure that the frequency derivative of $1/T_m$ is smaller at lower frequencies. This illustrates that as $f \rightarrow 0$, a static freezing temperature is approached. Further, the relaxation time is distributed over a certain temperature region. As the temperature is lowered, τ increases and at a critical value $T_m = T_f$, τ becomes extremely large and consequently the stable polarization is frozen to the glassy state [16]. The fitting of Vogel–Fulcher relation with experimental data suggests that this mechanism can also be employed to explain the relaxor behaviour in such ceramics.

4. Conclusion

Polycrystalline sample of nanosized $\text{Na}_2\text{Mo}_2\text{O}_7$ prepared by solid-state reaction technique has been found to have single-phase spinel cubic structure. Vibrational (Raman/FTIR) spectra are studied for the confirmation of the formation of compound, and also to observe their molecular structure at microscopic level. Complex impedance spectroscopy (CIS) analysis has provided evidence for the existence of both grain (bulk) and grain boundary effects in the material that are separated in the frequency domain of the impedance spectrum. The experimental data of Vogel–Fulcher relation suggest that this mechanism can be employed to explain the relaxor behaviour in $\text{Na}_2\text{Mo}_2\text{O}_7$ ceramics.

References

- [1] T Mathews, D Krishnamurthy and T Gnanasekaran, *J. Nucl. Mater.* **247**, 280 (1997)
- [2] K C Emregül and A A Aksüt, *Corros. Sci.* **45**, 2415 (2003)
- [3] S Sharma, R N P Choudhary and S R Shanigrahi, *Mater. Lett.* **40**, 134 (1999)
- [4] S Mukherjee, M Chakraborty, A K Panda, S C Bhattacharya and S P Moulik, *Coll. Surf. A: Physicochem. Engg. Aspects* **388**, 1 (2011)
- [5] Y Ding, N Hou, N Chen and Y Xia, *Rare Metals* **25**, 316 (2006)
- [6] K Gesi, *J. Phys. Soc. Jpn* **53**, 3850 (1984)
- [7] S N Choudhary and R N P Choudhary, *Mater. Lett.* **34**, 411 (1998)
- [8] O P Barinova, S V Kirsanova, *Glass Ceram.* **65**, 362 (2008)
- [9] E Wu, POWD: An interactive powder diffraction data interpretation and indexing programme, Ver. 2.5, School of Physical Science, Flinders University of South Australia, Bedford Park, SA 5042, Australia
- [10] P Scherrer, *Gottin Nachricht* **2**, 98 (1918)
- [11] G D Saraiva, W Paraguassu, M Maczka, P T C Freire, J A Lima Jr, C W A Paschoal, J Mendes Filho and A G Souza Filho, *J. Raman Spectrosc.* **39**, 937 (2008)
- [12] M Balkanski, R F Wallis and E Haro, *Phys. Rev. B* **28**, 1928 (1983)
- [13] C Bharti, A Dutta and T P Sinha, *Mater. Res. Bull.* **43**, 1246 (2008)
- [14] S K Bera, S K Barik, R N P Choudhary and P K Bajpai, *Bull. Mater. Sci.* **35**, 47 (2012)
- [15] K Prasad, K Kumari, K P Chandra, K L Yadav and S Sen, *Solid State Commun.* **144**, 42 (2007)
- [16] P Bonneau, O Garnier, G Calvarin, E Hussin, J R Gavari, A W Heiwat and A Morell, *J. Solid State Chem.* **91**, 350 (1991)